AD-A276 963

NAWCWPNS TP 8185

Wavelet Transform of Fixed Pattern Noise in Focal Plane Arrays

by
Dr. Gary Hewer
and
Wei Kuo
Intercept Weapons Department

FEBRUARY 1994

**NAVAL AIR WARFARE CENTER WEAPONS DIVISION
CHINA LAKE, CA 93555-6001**

94-08379

94 3 14 087

Naval Air Warfare Center Weapons Division

FOREWORD

This report summarizes our joint research on the infrared fixed pattern noise on a microbolometer. The report demonstrates that Daubechies wavelets filter the noise in a predictable manner and presents a new approximate model for the noise, namely, power-law shot noise. The work was performed at the Naval Air Warfare Center Weapons Division, China Lake, Calif., during 1993 under Program Element Task Area RA11C12, Work Units 129295.

This report was reviewed for technical accuracy by Larry Peterson.

Approved by
DR. J. A. WUNDERLICH, *Head*
Intercept Weapons Department
7 February 1994

Under authority of
D. B. McKINNEY
RAdm., U.S. Navy
Commander

Released for publication by
S. HAALAND
Deputy Commander for Research and Development

REPORT DOCUMENTATION PAGE

1. AGENCY USE ONLY (Leave blank)	2. REPORT DATE	3. REPORT TYPE AND DATES COVERED
	February 1994	Final; 1993

4. TITLE AND SUBTITLE
Wavelet Transform of Fixed Pattern Noise in Focal Plane Arrays

5. FUNDING NUMBERS
P. E. Task Area RA11C12,
Work Units 129295

6. AUTHOR(S)
G. A. Hewer and Wei Kuo

7. PERFORMING ORGANIZATION NAME(S) AND ADDRESS(ES)
Naval Air Warfare Center Weapons Division
China Lake, CA 93555-6001

8. PERFORMING ORGANIZATION REPORT NUMBER
NAWCWPNS TP 8185

9. SPONSORING/MONITORING AGENCY NAME(S) AND ADDRESS(ES)

10. SPONSORING/MONITORING AGENCY REPORT NUMBER

11. SUPPLEMENTARY NOTES

12A. DISTRIBUTION/AVAILABILITY STATEMENT
Approved for public release; distribution is unlimited.

12B. DISTRIBUTION CODE

13. ABSTRACT *(Maximum 200 words)*
(U) This report summarizes research on the infrared fixed pattern noise on a microbolometer. The report demonstrates that Daubechies wavelets filter the noise in a predictable manner and presents a new approximate model for the noise, power-law shot noise.

14. SUBJECT TERMS
fixed pattern noise, fractional Brownian motion, power-law shot noise, staring focal plane array, wavelets

15. NUMBER OF PAGES
25

16. PRICE CODE

17. SECURITY CLASSIFICATION OF REPORT	18. SECURITY CLASSIFICATION OF THIS PAGE	19. SECURITY CLASSIFICATION OF ABSTRACT	20. LIMITATION OF ABSTRACT
UNCLASSIFIED	UNCLASSIFIED	UNCLASSIFIED	UL

CONTENTS

ACKNOWLEDGMENTS

Acce_io·· For	
NTIS CRA&I	☑
DTIC TAB	☐
Unannounced	☐
Justification	

By

D: ib·

Dist

A-1

INTRODUCTION

In a series of seminal papers, Flandrin (References 1 and 2) and Tewfik et al. (References 3 through 5) proved that the Daubechies wavelets decorrelate or "whiten" a broad class of stochastic processes that have a 1/f-type spectra. Concurrently, Scribner et al. (References 6 through 9) have asserted that a major contributor to the fixed pattern nonuniformity observed on infrared staring arrays is the 1/f-type spectra associated with the sampled output of the individual pixels. Using measurement from an Amber 128-by-128 indium antimonide (InSb) staring array, Hewer and Kuo (References 10 and 11) combined these two results to demonstrate that the Daubechies wavelets do "whiten" the 1/f-type spectra as predicted. Hewer and Kuo also proposed fractional Brownian motion (fBm) as a stochastic process that could serve as a possible model for the spectra. The purpose of this note is to demonstrate that the predicted Daubechies wavelet filtering properties that were demonstrated for InSb can be extended to microbolometers.

In much of the physics and engineering literature, 1/f noise is characterized by a spectral family $F(\omega) \propto \dfrac{\sigma}{\omega^{\alpha}}$ $\sigma > 0$ in a neighborhood of the origin with $1 \leq \alpha \leq 3$. Flicker noise occurs when $\alpha = 1$, and $\alpha = 2$ is Brownian noise. The study of such processes is somewhat paradoxical, because for $\alpha = 1$ the spectrum is not integrable on the semi-infinite interval $[0, \infty)$. This suggests that the model implies infinite variance and therefore that the spectrum of the process apparently cannot exist. However, physical limitations of any experiment impose limits on the frequency range that can be measured. Moreover, the spectrum will not generally uniquely characterize a stochastic process. In Hewer and Kuo, fBm was proposed as a possible stochastic model, because it is compatible with the Daubechies filters and has several properties that match the structure of the measured pixel time series. In this paper another stochastic model is proposed that also has a 1/f spectral family. This new model, called power-law shot noise, was derived by Lowen and Teich (References 12 and 13).

In this note just enough detail is included to explain the terminology and relevant concepts. The interested reader can find more details and many references in Hewer and Kuo. The comprehensive review by Wornell (Reference 14) of the 1/f family of fractal processes and wavelets is recommended.

FRACTIONAL BROWNIAN MOTION

Mandelbrot and Van Ness (Reference 15) introduced the class of stochastic processes called fractional Brownian motion, which includes ordinary Brownian motion as a special case. Denoting the process as $B_H(t)$ it is a zero- mean non stationary stochastic process

that is indexed by a single scale parameter H. Here we assume that $B_H(0) = 0$ for convenience. The fBm covariance has the following form for $0 < H < 1$.

$$\text{cov}(B_H(t,s)) = E[B_H(t)B_H(s)] = \frac{\sigma^2}{2}(|s|^{2H} + |t|^{2H} - |t-s|^{2H})$$

When the index $H = 1/2$ the fBm is ordinary Brownian motion.

Several algorithms exist to simulate fBm. The Hosking algorithm (Reference 16) simulates fBm with the spectral family $\frac{1}{\omega^{2H+1}}$ and fractional Gaussian noise (fGn) with the spectral family $\frac{1}{\omega^{2d}}$. Here H denotes the Hurst coefficient and $H = d + 1/2$ with $|d| \leq \frac{1}{2}$. The correlation character of fGn strongly depends on H and is summarized as by Wornell (Reference 14) and Feder (Reference 17) as shown in Equation 1.

$$\begin{cases} d > 0 & \text{persistence} \\ d = 0 & \text{no correlation} \\ d < 0 & \text{anti-persistence} \end{cases} \tag{1}$$

POWER-LAW SHOT NOISE

Power-law shot noise, introduced by Lowen and Teich, is defined as follows. The shot noise is expressed as an infinite sum of power-law impulse response functions

$$I(t) = \sum_{j=-\infty}^{\infty} h(t - t_j)$$

where

$$h(t) = \begin{cases} K t^{-\beta} & 0 < A < t < B \\ 0 & \text{otherwise} \end{cases}$$

and the times t_j are random events from a homogeneous Poisson point process at a rate μ. The power spectral density $S(\omega)$ of the process approaches the constant value as $\omega \to 0$

$$S(\omega) \to \mu K^2 \frac{B^\alpha}{(\alpha/2)^2}$$

and as $\omega \to \infty$

$$S(\omega) \to \mu K^2 \Gamma^2(\frac{\alpha}{2})(\omega)^{-\alpha}$$

where $\Gamma(.,.)$ is the incomplete gamma function defined by

$$\Gamma(q,x) \equiv \int_x^\infty e^{-t} t^{q-1} dt \ .$$

The parameters A, B, K, α, β, and μ ($\alpha = 2(1-\beta)$) are deterministic and fixed.

When A > 0 and B < ∞ the density function for the amplitude will converge to a Gaussian distribution (I(t)$\rightarrow$Gaussian) with mean C_1 and variance C_2, which are defined as follows.

$$C_1 = \mu K \begin{cases} \left. (A^{1-\beta} - B^{1-\beta}) \middle/ (\beta-1), \right. & \beta \neq 1; \\ \ln \dfrac{B}{A}, & \beta = 1; \end{cases}$$

$$C_2 = \mu K \begin{cases} \left. (A^{1-2\beta} - B^{1-2\beta}) \middle/ (2\beta-1), \right. & \beta \neq 0.5; \\ \ln \dfrac{B}{A}, & \beta = 0.5; \end{cases}$$

DAUBECHIES WAVELETS

The wavelets $\varphi(t)$ introduced by Daubechies (Reference 18) are obtained from the scaling function $\phi(t)$, which is the solution of the two-scale difference equation (a dilation equation)

$$\phi(t) = \sum_k c_k \phi(2t - k).$$

If the coefficient sequence $\{c_k\}$ has only a finite number of nonzero terms, the wavelet $\varphi(t)$ has compact support. The sequence $\{c_k\}$ satisfies the following conditions, which are respectively a normalizing condition, an orthogonality condition (δ_{mn} is the discrete Dirac delta function), and a regularity or vanishing moment condition.

$$\sum c_k = \sqrt{2}, \quad \sum c_k c_{k-2m} = 2 \delta_{0m}, \quad \sum (-1)^k k^m c_k = 0, \ m = 0, 1, \cdots, p-1 \tag{2}$$

The wavelet equation is constructed from the sequence $\{c_k\}$ by the quadrature mirror condition

$$\varphi(t) = \sum_k (-1)^k c_{1-k} \phi(2t - 1).$$

The Haar wavelet has compact support is quite simple and is defined as follows.

$$\varphi(t) = \begin{cases} +1 & 0 \le t < 1/2 \\ -1 & 1/2 \le t < 1 \\ 0 & \text{otherwise} \end{cases}$$

and the scaling function is

$$\phi(t) = \begin{cases} +1 & 0 \le t < 1 \\ 0 & \text{otherwise} \end{cases}$$

Compactly supported Daubechies wavelets will be denoted by D_p with $p = 1, 2, \ldots$ with D_1 denoting the Haar wavelet. The coefficients for the first Daubechies wavelet D_2 are

$$c_0 = \frac{(1+\sqrt{3})}{4\sqrt{2}} \qquad c_1 = \frac{(3+\sqrt{3})}{4\sqrt{2}}$$

$$c_2 = \frac{(3-\sqrt{3})}{4\sqrt{2}} \qquad c_3 = \frac{(1-\sqrt{3})}{4\sqrt{2}}$$

The compactly supported Daubechies wavelets form an orthonormal basis for $L^2(R)$, which means that any function that is a member of $L^2(R)$ can be expanded into a wavelet series instead of a Fourier series. A function that is a member of $L^2(R)$ has "finite power" and can be expanded into a series using the sequence of wavelets $\left\{ \sqrt{2^j} \varphi(2^j t - m) \right\}$ as the basis functions. Moreover, for some wavelets all translates and dilates of $\varphi(t)$ are mutually orthogonal using the inner product $\langle * \rangle$

$$\left\langle \sqrt{2^k} \varphi(2^k t - l), \sqrt{2^j} \varphi(2^j t - m) \right\rangle = \delta_{jk} \delta_{ml}.$$

The discrete wavelet coefficients that represent the expansion in the scaling functions are called the approximation coefficients $a_j(n)$

$$a_j[n] = \left\langle f(t), \sqrt{2^j} \phi(2^j t - n) \right\rangle = \sqrt{2^j} \int_{-\infty}^{\infty} f(t) \phi(2^j t - n) dt,$$

where f(t) is any function in $L^2(R)$. The wavelet expansion coefficients are called the detail coefficients $d_j(n)$, because they represent the difference between two successive approximations and are computed as follows.

$$d_j[n] = \left\langle f(t), \sqrt{2^j} \varphi(2^j t - n) \right\rangle = \sqrt{2^j} \int_{-\infty}^{\infty} f(t) \varphi(2^j t - n) dt$$

For any finite integer J, $\left\{ \sqrt{2^J} \phi(2^J t - m) \cup \sqrt{2^J} \varphi(2^J t - m) \right\}$ is an orthonormal basis for $L^2(R)$. Thus, any function f(t) in $L^2(R)$ can be written as the nonhomogeneous wavelet infinite series

$$f(t) = \sqrt{2^J} \sum_{m=-\infty}^{m=\infty} a_j(m)\phi(2^J t - m) + \sum_{j=J}^{\infty} \sum_{m=-\infty}^{m=\infty} \sqrt{2^J} d_j(n)\varphi(2^J t - m).$$

This series expansion is called a multiresolution decomposition of f(t). The decomposition is multiresolution, because the approximation coefficients and the detail coefficients are computed at successively different scales indexed by j. Note the different role played by the approximation coefficients (a scales) and the detail coefficients (d scales) in the expansion.

SMOOTHING OF 1/f SIGNALS

Wornell (Reference 14) illustrates extracting a 1/f signal from a background of additive stationary white noise. Donoho (Reference 19) has proposed wavelet shrinkage as an attractive alternative for the same purpose. His method shrinks noisy wavelet coefficients via thresholding. The method has theoretical properties that exceed anything previously known. His method applies a soft-threshold nonlinearity $\eta_t(w) = sgn(w)(|w|-t)_+$ with threshold t to each empirical sample value w in the wavelet transform d scales. After thresholding the wavelet transform is inverted, yielding the smoothed data. Applying the soft threshold continuously shrinks the empirical coefficients in the d scales to zero and thus removes the noise.

SIMULATED fBm, 1/f SHOT NOISE, AND CAMERA TEST RESULTS

Figures 1 through 12 use simulated fBm to illustrate some important stochastic estimates that will be applied to the infrared camera data. A complete set of references and relevant concepts is contained in the SPIE paper or technical report by Hewer and Kuo (References 10 and 11). Although these results and figures are similar to those found in Hewer and Kuo, they are included for completeness and for a direct comparison with the power-law shot noise simulation and the Honeywell microbolometer data.

Figure 1 is a sample path containing 3000 points of an anti-persistent fBm with the spectral family $\frac{1}{\omega^{2H+1}}$ for H = 0.1. These samples were generated using the Hosking algorithm.[16] Figure 2 shows the corresponding periodograms, a log-log plot of the periodogram X(ω) versus the frequency variable ω. The periodogram X(ω) is the modulus of the Fourier transform $\Im(x(n))$ of the discrete sequence $\{x_0, \cdots, x_{N-1}\}$

$$X(\omega) = \left(\frac{1}{N}\right)\Im(x(n))\Im(x(n))^*.$$

where N is the total number of samples and ( )* is the complex conjugate. The index H can be estimated from the slope of the dotted line. It is the least squares fit to the lower frequencies on the log-log plot of the periodogram.

Figure 3 is the corresponding correlation, which clearly exhibits slow decay with hyperbolic shape and a significant dependence between observations well separated in time. The next figure is a plot of the correlation function for the increments. The increments are obtained by applying the differencing operator ∇ to the fBm sequence x(n), which yields the derived sequence

$$\nabla x(n) = x(n) - x(n-1).$$

Because the increments of fBm are fGn, the lagged correlation coefficients will all be positive for persistence and negative for anti-persistence. Because Figure 1 is a sample of the anti-persistent case, the coefficient is negative as expected.

Figure 5 shows quantile-quantile (Q-Q) plots of the increments. A Q-Q plot can be used to compare the degree of agreement between two empirical distributions or to compare the empirical quantiles with the quantiles from an ideal distribution. A Gaussian Q-Q plot is a plot of the ordered data y_i from the sample $\{x_0, \cdots, x_{N-1}\}$ versus the normal quantiles $y_{p_i} = \Phi^{-1}(p_i)$, where $p_i = (i - \frac{1}{2})/N$, $i = 1, 2, \cdots, N$, and Φ^{-1} is the inverse of the standard normal distribution (Reference 20). If the shape of the marginal distributions for the increments is approximately normal, even in the tails, then the empirical quantile sample values will approximate the normal line. The approximation in Figure 5 is linear even in the tails, so the Gaussian hypothesis for the marginal distribution as simulated by the Hosking fBm model is reasonable.

Figure 7 is a plot of the fourth scale detail coefficients $d_4(n)$ for the Daubechies D_{10} wavelet. The next figure is the corresponding correlation. As expected, the Daubechies wavelet decorrelates or whitens the fBm process. The reason for this fortuitous transformation is given by Flandrin (Reference 2) and Tewfik and Kim (Reference 5) and is related to the vanishing moment properties defined in Equation 2. The survey by Wornell should be consulted for more discussion of the correlation structure of the wavelet coefficients. Even though the noise is not Gaussian, Donoho's wavelet shrinkage algorithm in S+WAVELETS was applied to the fBm signal with satisfactory results as shown in Figure 8.

Figure 9 is the same fBm sample as in Figure 1 with the addition of stationary white noise. The additive noise has a variance of 3.691, which yields a signal-to-noise ratio of zero decibels. The same processing sequence is reapplied to the signal in Figure 9, and the results are shown in Figures 10 through 16. These examples show that the processing is "robust" to additive white noise. Figure 10 demonstrates that the additive white noise clearly does not affect the low frequencies where the 1/f noise dominates but does contribute to the high frequencies. The one surprise is that the wavelet shrinkage produces a smoother curve in Figure 16 than in Figure 8. Figures 11 through 15

demonstrate that the estimation techniques and Daubechies filters are resistant to additive white noise.

The 1/f shot noise presentation in Figures 17 through 24 parallels the fBm presentation in Figures 1 through 8. The 1/f shot noise is simulated with parameter values $\beta = 0.4$, $K = 1$, $\mu = 1$, $A = 0.01$, and $B = 50$. The sample path in Figure 17 is a vector of length 5000 with a sampling interval of 0.2. The notation for fBm and the 1/f shot noise is consistent with the literature. The key relation between the Hurst coefficient H for the fBm and the parameter beta the power-law shot noise is $H = 0.5 - \beta$. The estimate for beta obtained in Figure 18 is 0.390567, which is consistent with the estimates for fBm. The remaining figures for this case do not exhibit any unexpected results.

Figures 25 through 40 are an application of the estimation techniques and the Daubechies filter applied to the camera data. These results are representative and not in way special or atypical. Figure 25 represents 7000 samples with a 54 Hertz sampling rate from a single pixel measured by a 128x128 Amber AE 4128 InSb focal plane array. More details on test conditions are found in Hewer and Kuo.[11] The estimate 0.158828 for H in Figure 26 yields an estimate for the spectral $F(\omega) = \frac{1}{\omega^{2H+1}}$ exponent of 1.317. Figures 27 through 32 are consistent with their simulated counterparts and with the hypothesis that the temporal pixel noise is a member of the 1/f spectral family.

Figure 33 represents 8046 samples from a single pixel measured by a Honeywell microbolometer. A bolometer is an infrared detector that measures absorbed, incident infrared radiation by a voltage change in electrical resistance due to a non equilibrium temperature differential. The data featured were provided by the Naval Research Laboratory in Washington., D. C. The images are from a Honeywell uncooled microbolometer 336-by-165 IR sensor in the 8- to 12-micron spectral band. The data are looking at an extended blackbody source at 25°C through an f1.1 optic with 80% transmission. The data are digitized to 256 bit accuracy with a 33-millisecond frame time. More information on the Honeywell microbolometer can be found in Gallo et al. (Reference 21) and Wood (Reference 22). Again, the results are consistent with their parallel panels for the Amber camera and the simulated signals.

CONCLUSIONS

In this note the Daubechies wavelets have again filtered and decorrelated the fixed pattern noise as predicted by the theory of wavelet transforms, when applied to random signals with a decaying correlation structure. Also a simulated example demonstrate that power-law shot noise is consistent with the empirical data analysis

REFERENCES

1. P. Flandrin. "On the Spectrum of Fractional Brownian Noise," *IEEE Trans. on Information Theory*, Vol. 36 (1989), pp. 197-99.

2. ----------. "Wavelet Analysis and Synthesis of Fractional Brownian Noise," *IEEE Trans. on Information Theory*, Vol. 38,(1992), pp. 910-916.

3. M. Deriche and A. H. Tewfik. "Maximum Likelihood Estimation of the Parameters of Discrete Fractionally Differenced Gaussian Noise Process," *IEEE Trans. on Signal Processing*, Vol. 41 (1993), pp. 2977-89.

4. ----------. "Signal Modeling With Filtered Discrete Fractional Noise Processes," *IEEE Trans. on Signal Processing*, Vol. 41 (1993), pp. 2839-49.

5. A. H. Tewfik and M. Kim. "Correlation Structure of the Discrete Wavelet Coefficients of Fractional Brownian Motion," *IEEE Trans. on Information Theory*, Vol. 38 (1992), pp. 904-909.

6. D. A. Scribner, M. R. Kruer, C. J. Gridley, and K. Sarkady. "Measurement, Characterization, and Modeling of Noise in Staring Focal Plane Arrays," *SPIE Proceedings Vol. 782 Infrared Sensors and Sensor Fusion* (1987), pp. 147-160.

7. ----------. "Physical Limitations to Nonuniformity Correction in IR Focal Plane Arrays," *SPIE Vol. 865 Focal Plane Arrays: Technology and Applications* (1987), pp. 185-202.

8. D. A. Scribner, K. A. Sarkady, M. R. Kruer, and C. J. Gridley. "Test and Evaluation of Stability in IR Staring Focal Plane Arrays After Nonuniformity Correction," *SPIE Proceedings Vol. 1108 Test and Evaluation of Infrared Detectors and Arrays* (1989), pp. 255-64.

9. D. A. Scribner, K. A. Sarkady, J. T. Caulfield, M. R. Kruer, G. Katz, C. J. Gridley, and Charles Herman. "Nonuniformity Correction for Staring IR Focal Plane Arrays Using Scene-Based Techniques," *SPIE Proceedings Vol. 1308 Infrared Detectors and Focal Plane Arrays* (1990), pp. 224-33.

10. G. A. Hewer and Wei Kuo. "Wavelet Transform of Fractional Brownian Motion for Infrared Focal Plane Arrays," *SPIE Proceedings Volume 1961* (1993), pp. 305-15.

11. Naval Air Warfare Center Weapons Division. *Fractal Brownian Motion, Wavelets, and Infrared Detector Noise*, by G. A. Hewer and Wei Kuo. China Lake, Calif., NAWCWPNS, March 1993. (NAWCWPNS TP 8103, publication UNCLASSIFIED.)

12. Steven B. Lowen and Malvin C. Teich. "Power-Law Shot Noise," *IEEE Trans. on Information Theory*, Vol. 36, No. 6 (Nov. 1990), pp. 1302-18.

13. ----------. "Generalized 1/f Shot Noise," *Electronics Letters*, Vol. 25, No 16 (3 August 1989), pp. 1072-74.

14. Gregory W. Wornell. "Wavelet-Based Representation for the 1/f Family of Fractal Processes," *Proceedings of the IEEE*, Vol. 81 (1993), pp. 1428-50.

15. Benoit Mandelbrot and John W. Van Ness. "Fractional Brownian Motions, Fractional Noises and Applications," *SIAM Review*, Vol. 10, No. 2 (1988), pp. 422-37.

16. R. M. Hosking. "Modeling Persistence in Hydrological Time Series Using Fractional Differencing," *Water Resources Research*, Vol. 20 (1984), pp. 1898-1908.

17. Jens Feder. *Fractals*. San Francisco, Plenum Press, 1988.

18. Ingrid Daubechies. *Ten Lectures on Wavelets*. CBSM-NSF Regional Conference Series in Applied Mathematics, Vol. 60, Society for Industrial and Applied Mathematics, Philadelphia, 1992.

19. D. L. Donoho. "Wavelet Shrinkage and W. V. D.: A 10 Minute Tour," in *Progress in Wavelet Analysis and Applications*, Y. Meyer and S. Roquies, eds. Cedex, France, Editions Frontieres, 1993.

20. R. Gnanadesikan. *Methods for Statistical Data Analysis of Multivariable Observations*. New York, Wiley, 1977.

21. M. A. Gallo, D. S. Willits, R. A. Lubke, and E. C. Thiede. "Low Cost Uncooled IR Sensor for Battlefield Surveillance," *SPIE Vol. 2020 Infrared Technology XIX* (1993), pp. 351-62.

22. R. A. Wood, "Uncooled Thermal Imaging With Monolithic Silicon Focal Planes," *SPIE Vol. 2020 Infrared Technology XIX* (1993), pp. 322-29.
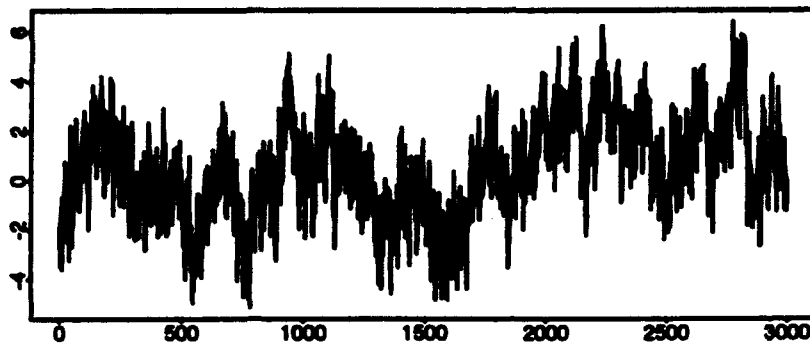
FIGURE 1. fBm With d = 0.4 (H = 0.1).
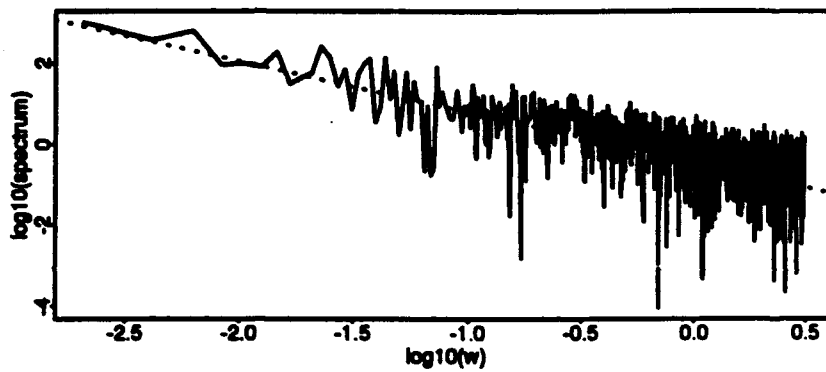
FIGURE 2. Periodogram of Figure 1. Estimated H is
0.122461.
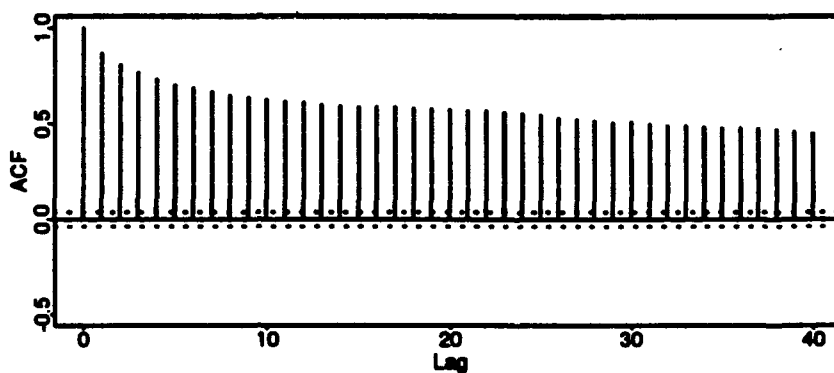
FIGURE 3. Correlation Function of Figure 1.
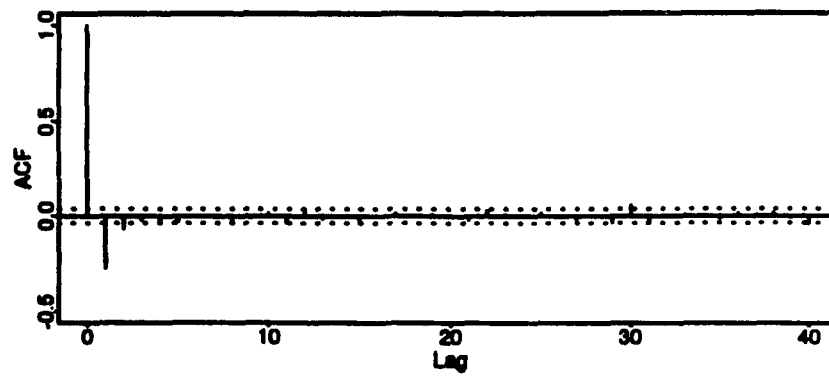
FIGURE 4. Correlation Function of Increment of Figure 1.
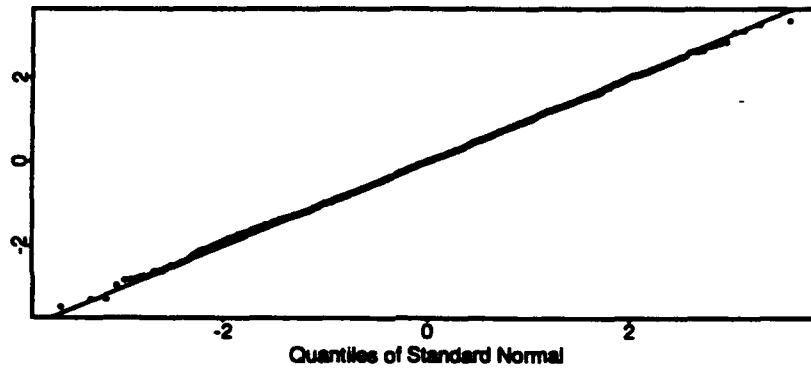
FIGURE 5. Normal Q-Q Plot of Increment of Figure 1.
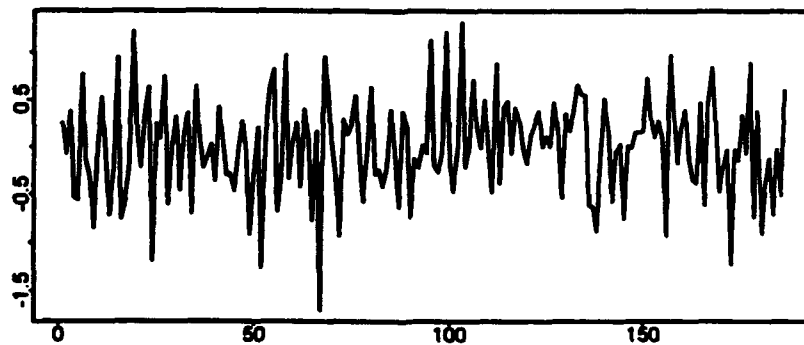
FIGURE 6. Daubechies 10 Wavelet d Scale 4 of Figure 1.
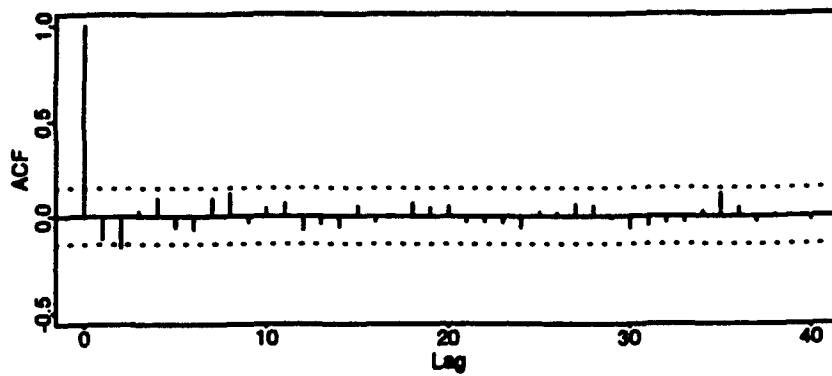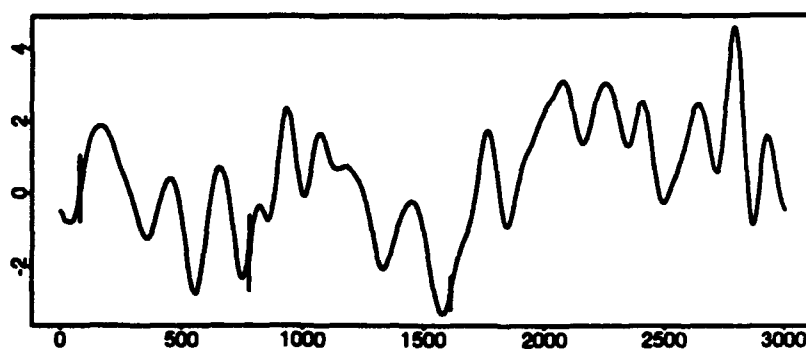
FIGURE 7. Correlation Function of Figure 6.
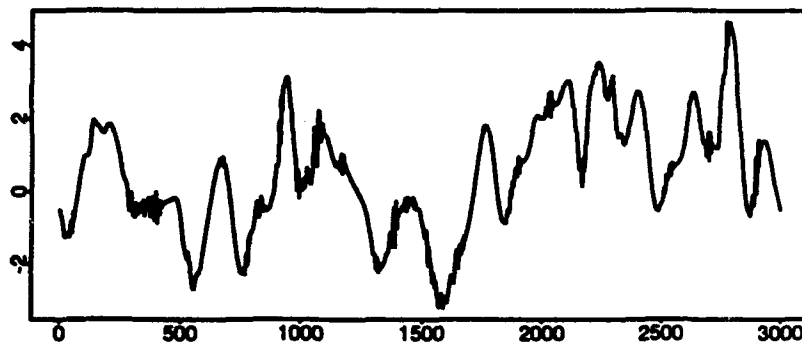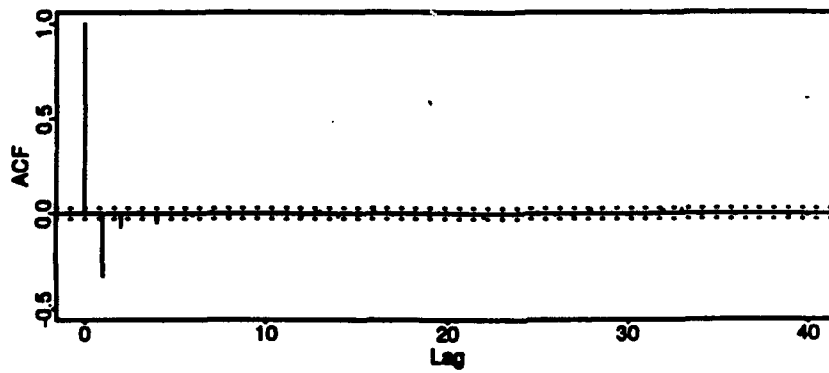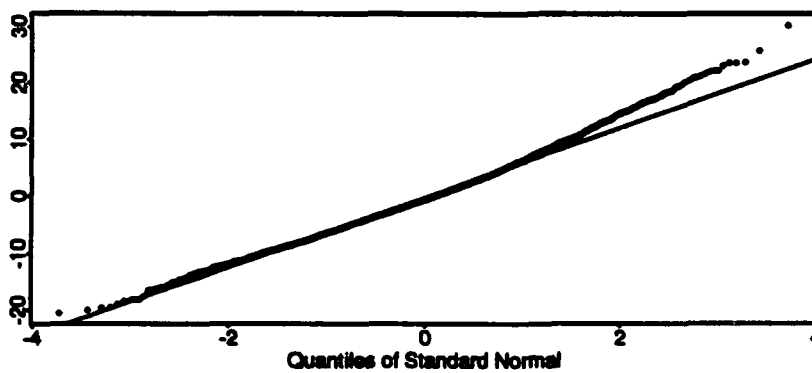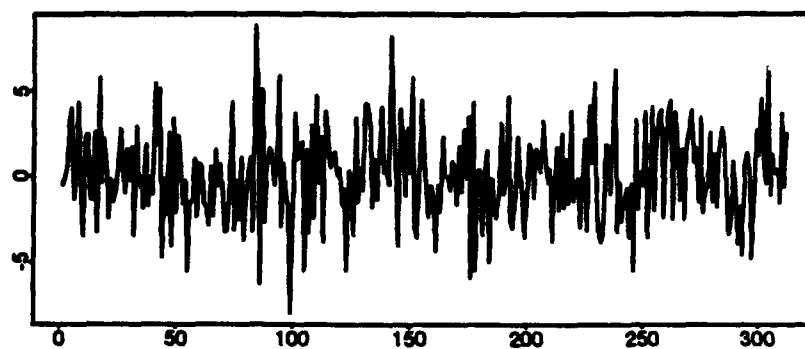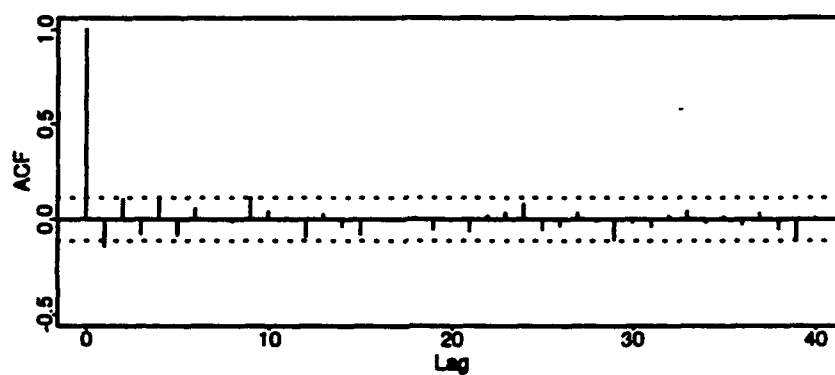

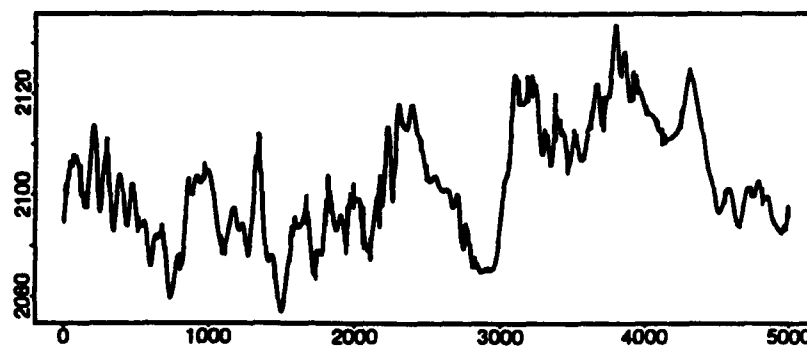FIGURE 8. Wavelet Shrinkage of Figure 1.
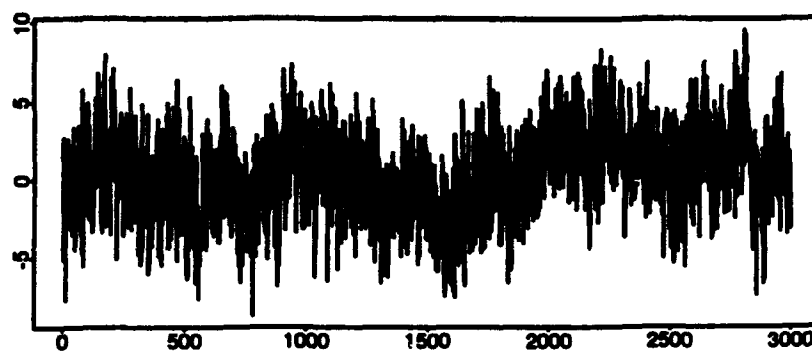
FIGURE 9. Figure 1 Plus White Noise With Variance
3.6913 (SNR = 0 dB).
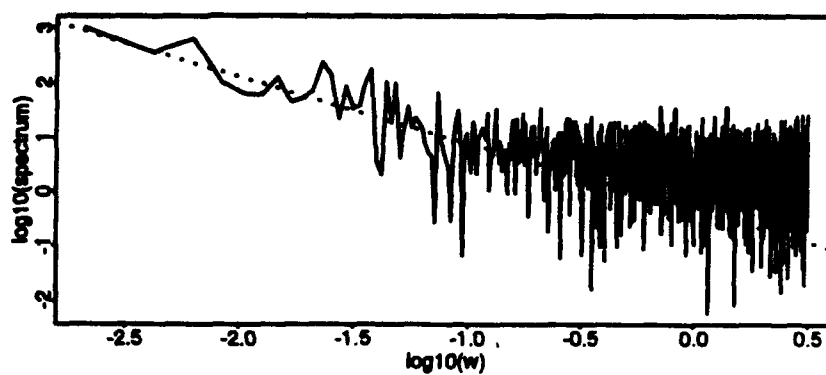
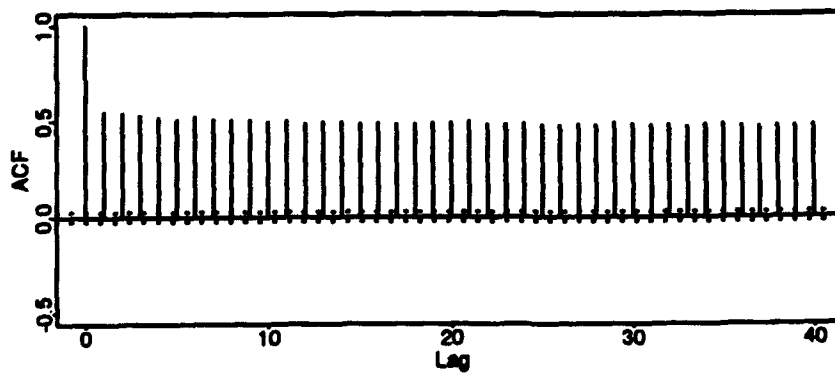FIGURE 10. Periodogram of Figure 9. Estimated H is 0.107295.
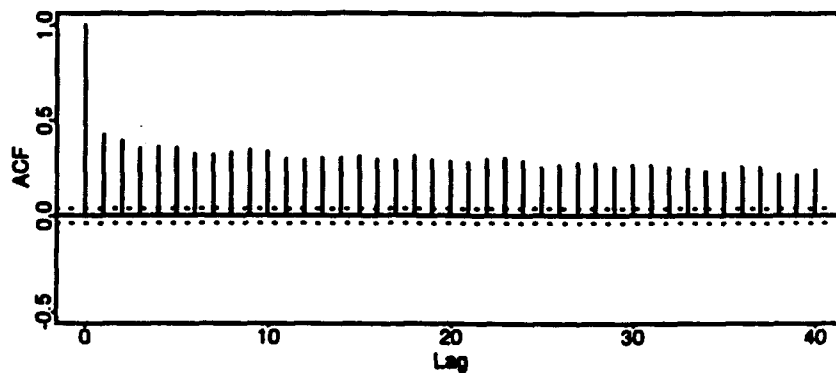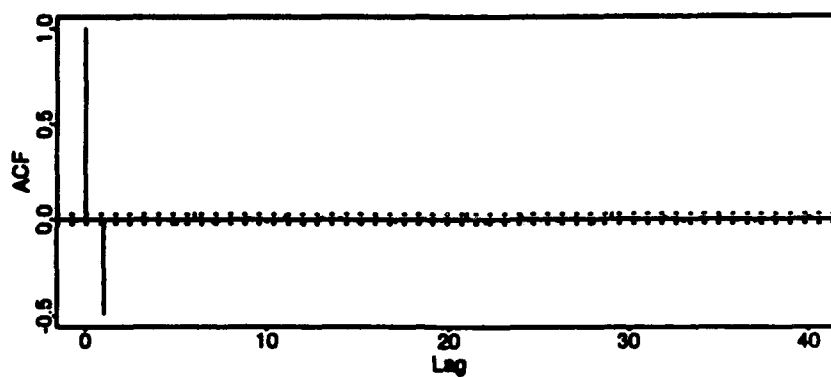

FIGURE 11. Correlation Function of Figure 9.
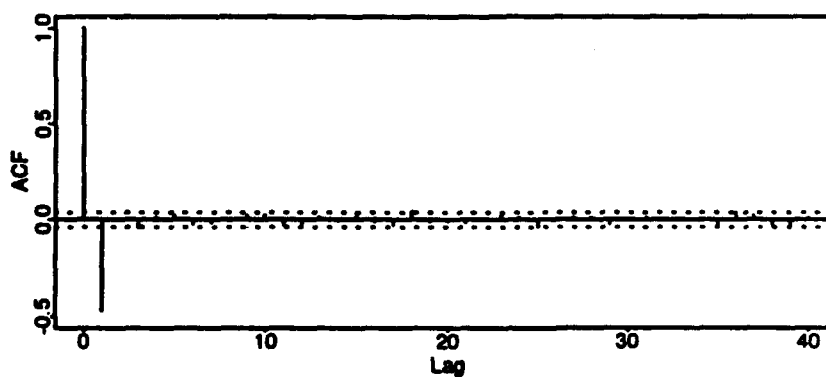
FIGURE 12. Correlation Function of Increment of Figure 9.
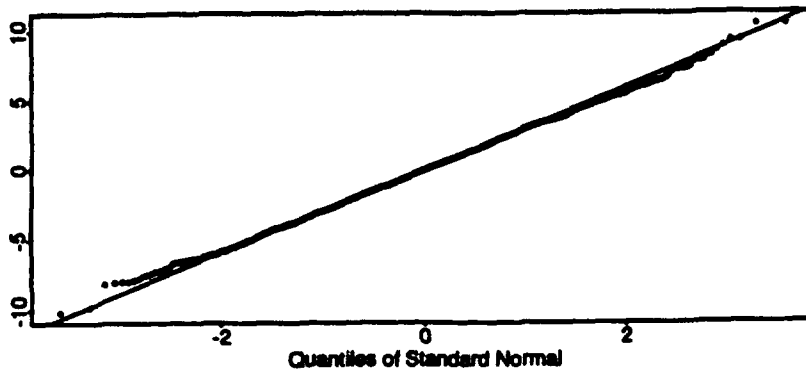
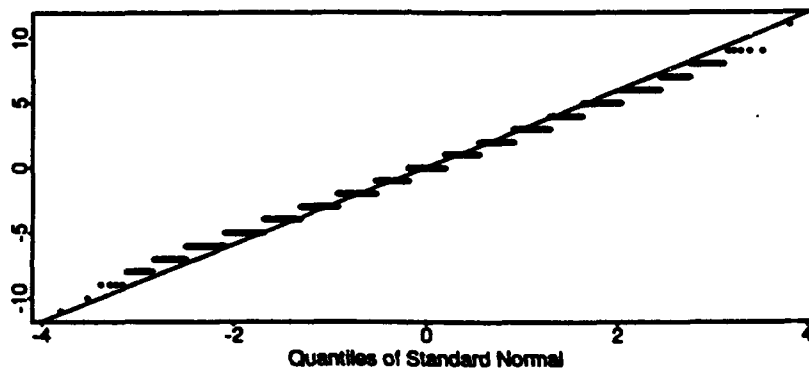FIGURE 13. Normal Q-Q Plot of Increment of Figure 9.
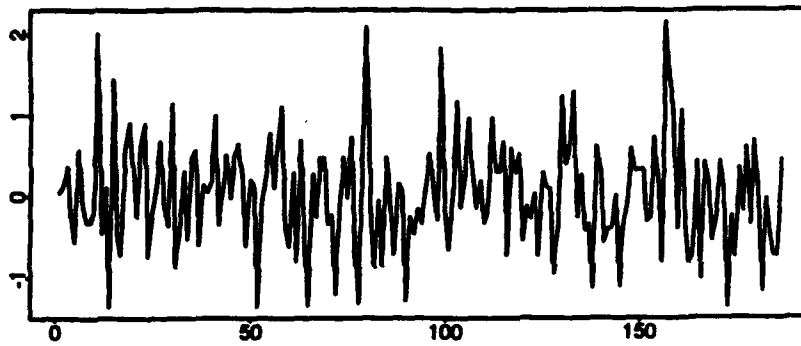
FIGURE 14. Daubechies 10 Wavelet d Scale 4 of Figure 9.
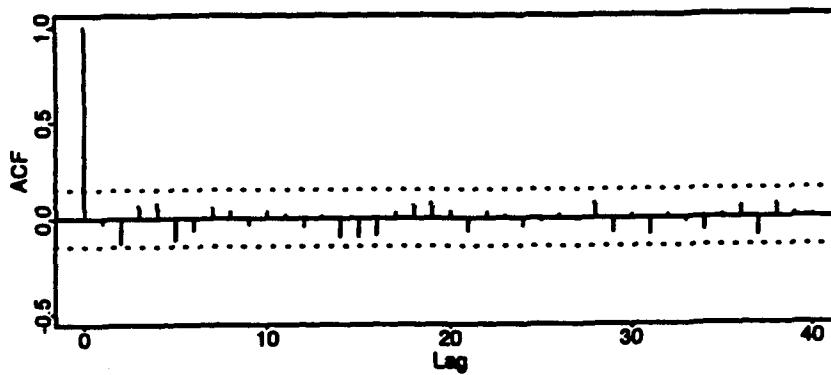
FIGURE 15. Correlation Function of Figure 14.

FIGURE 16. Wavelet Shrinkage of Figure 9.
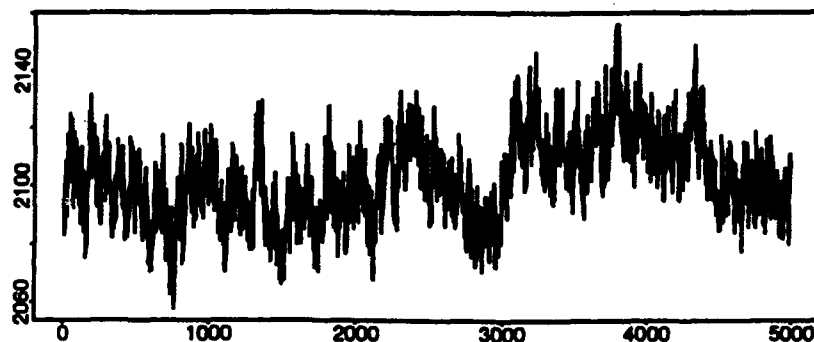
FIGURE 17. 1/f Shot Noise With d = 0.4 (H = 0.1).
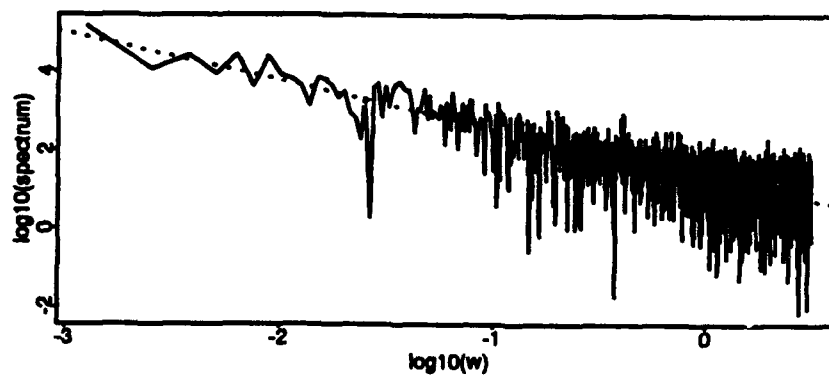
FIGURE 18. Periodogram of Figure 17. Estimated H is 0.109433.
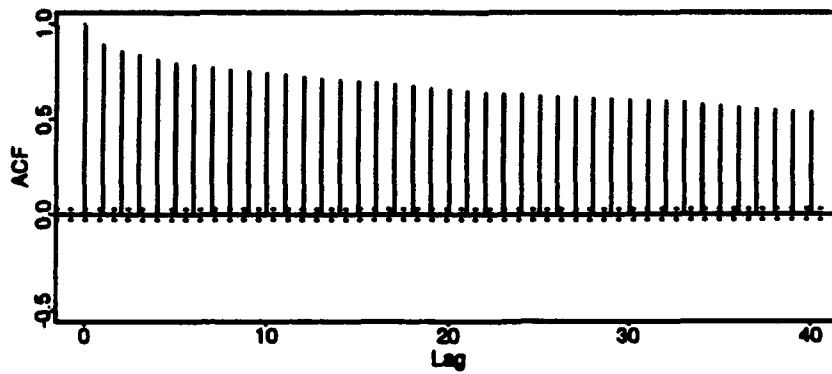
FIGURE 19. Correlation Function of Figure 17.

FIGURE 20. Correlation Function of Increment of Figure 17.
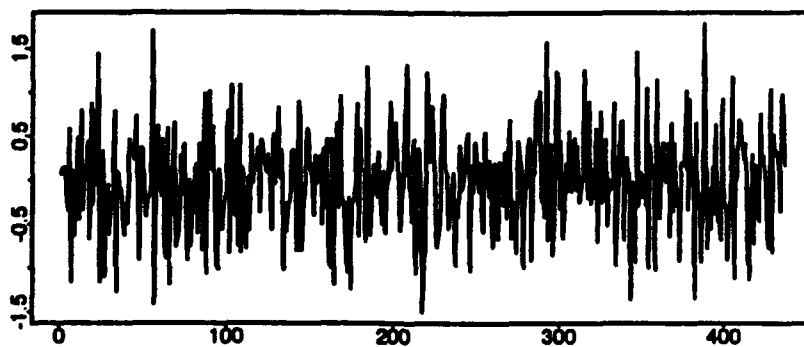

FIGURE 21. Normal Q-Q Plot of Increment of Figure 17.

18

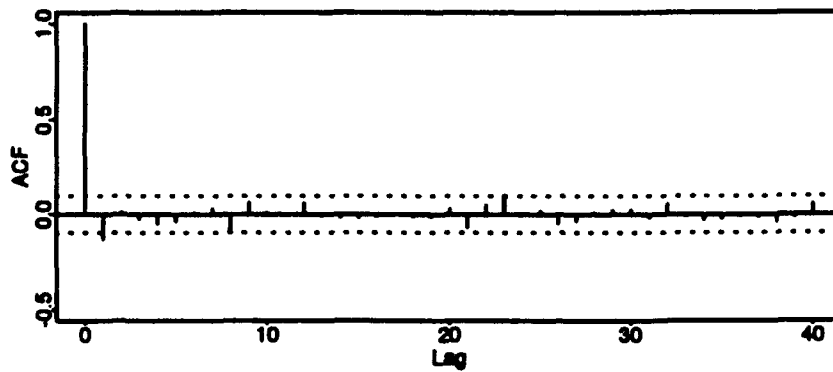FIGURE 22. Daubechies 10 Wavelet d Scale 4 of
Figure 17.

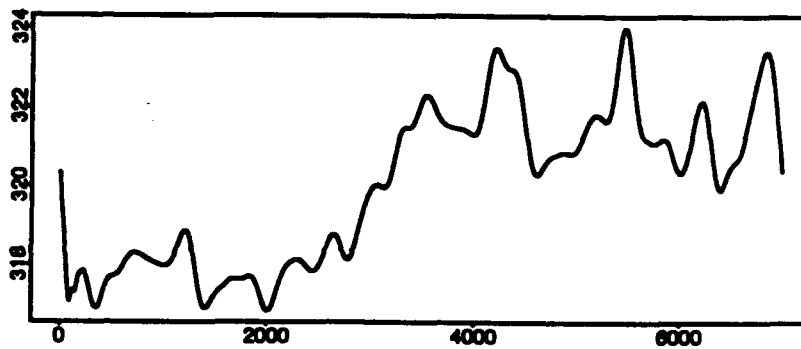FIGURE 23. Correlation Function of Figure 22.

FIGURE 24. Wavelet Shrinkage of Figure 17.
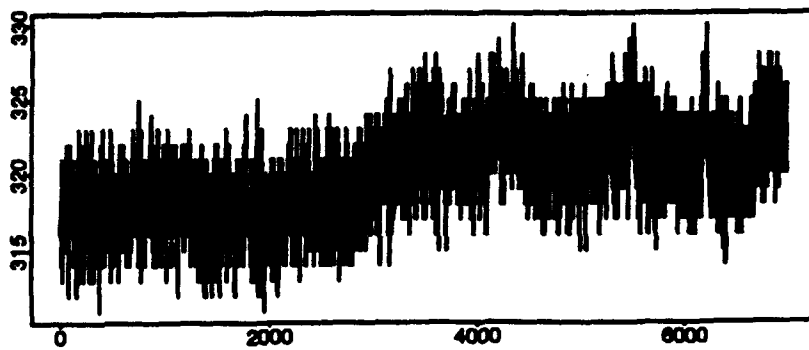
FIGURE 25. 54-Hertz Amber Camera Data, Pixel (8,8).
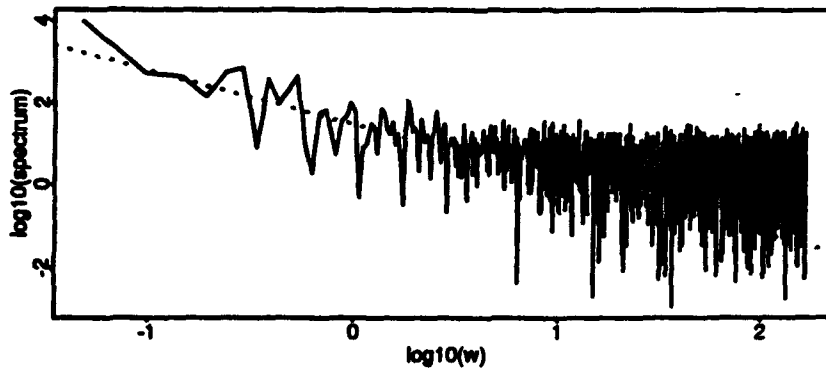
FIGURE 26. Periodogram of Figure 25. Estimated H is 0.158828.

FIGURE 27. Correlation Function of Figure 25.

20

FIGURE 28. Correlation Function of Increment of Figure 25.

FIGURE 29. Normal Q-Q Plot of Increment of Figure 25.

FIGURE 30. Daubechies 10 Wavelet d Scale 4 of Figure 25.

FIGURE 31. Correlation Function of Figure 30.
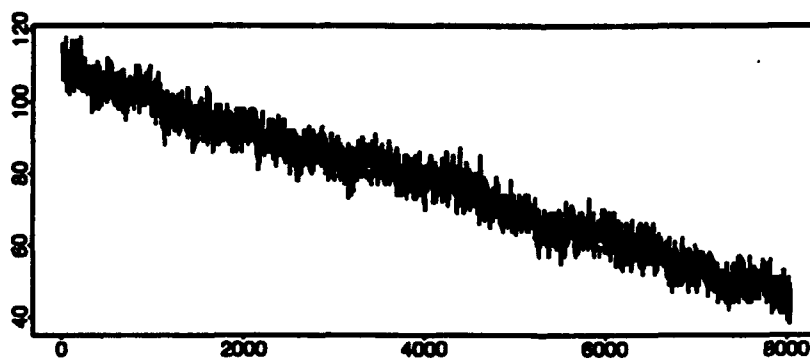

FIGURE 32. Wavelet Shrinkage of Figure 25.

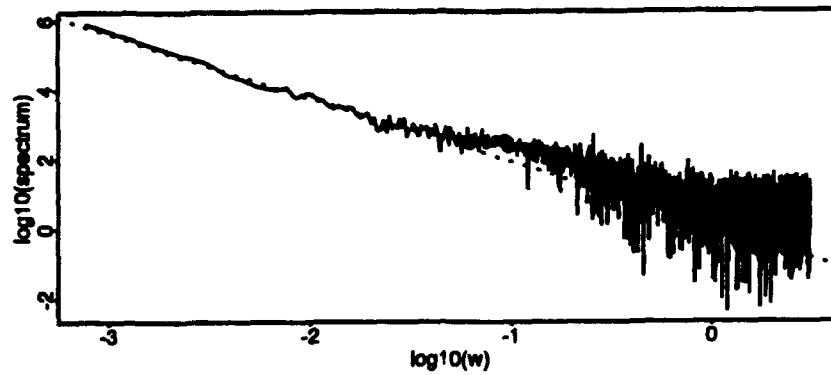FIGURE 33. Honeywell Uncooled Microbolometer Camera Data, Pixel (100,1).

FIGURE 34. Periodogram of Figure 33. Estimated H is 0.42459.
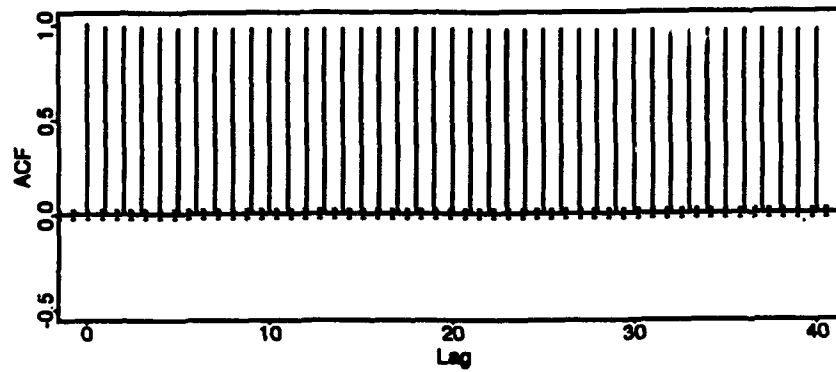
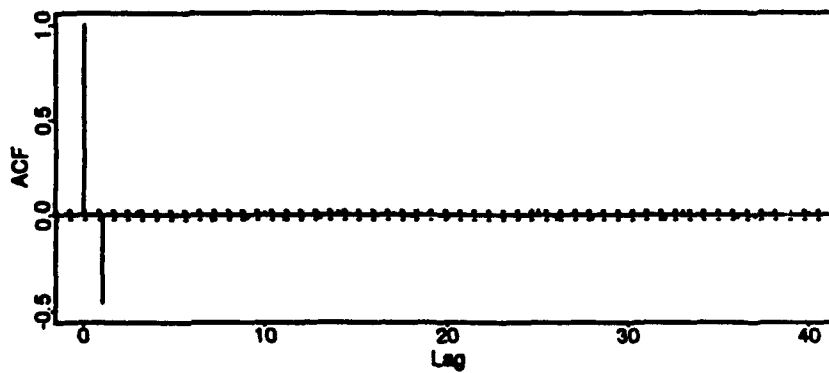

FIGURE 35. Correlation Function of Figure 33.

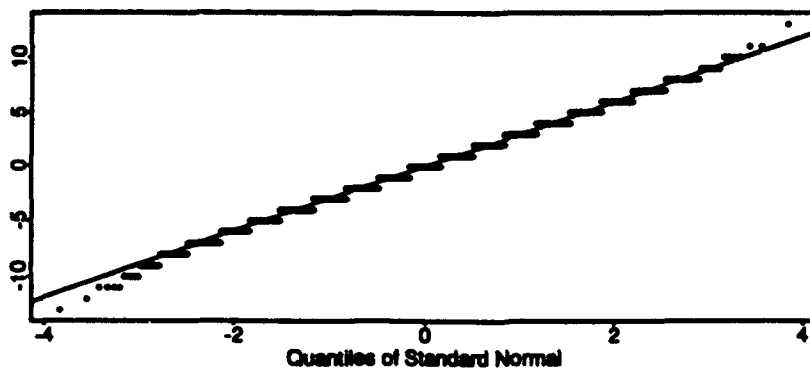FIGURE 36. Correlation Function of Increment of Figure 33.

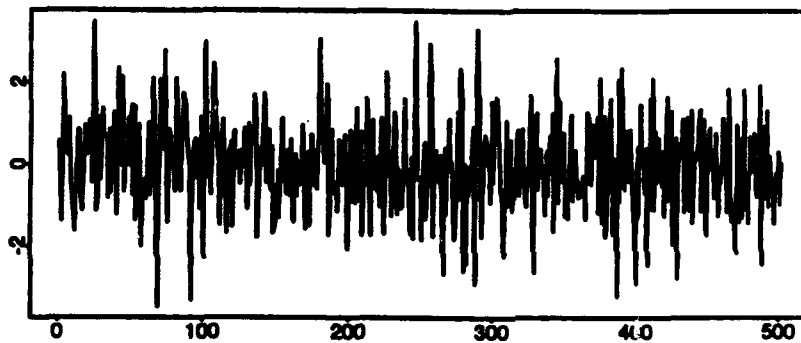FIGURE 37. Normal Q-Q Plot of Increment of Figure 33.

FIGURE 38. Daubechies 10 Wavelet d Scale 4 of
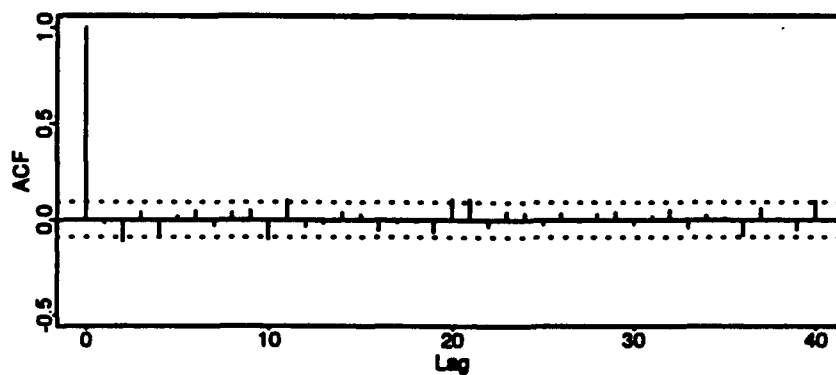Figure 33.
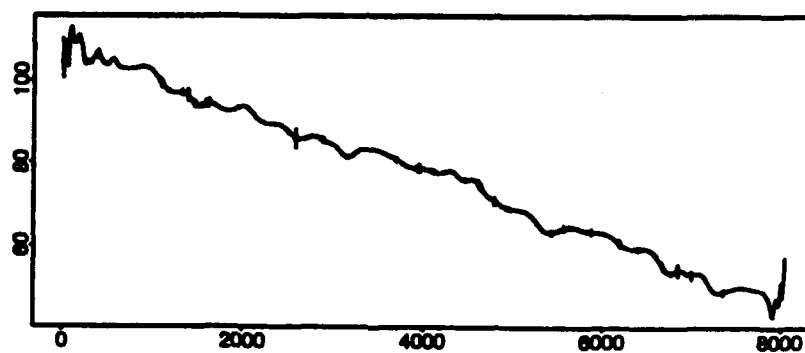

FIGURE 39. Correlation Function of Figure 38.

24

FIGURE 40. Wavelet Shrinkage of Figure 33.

INITIAL DISTRIBUTION

1 Naval Air Systems Command, Arlington (AIR-540th, R. Habayeb)
6 Chief of Naval Research, Arlington
    OCNR-311
      Dr. J. Abrahams (1)
      Dr. N. Gerr (1)
      W. J. Miceli (1)
      Dr. M. Schlesinger (1)
      E. Wald (1)
    OCNR-442E, D. Siegel (1)
1 Office Of Naval Research Europe (Dr. R. Ryan)
2 Naval Command Control and Ocean Surveillance Center, RDT&E Division, San Diego
    Code 632, Dr. M. Shensa (1)
    Code 7601T, Dr. K. Bromely (1)
1 Naval Postgraduate School, Monterey (Code EC/GL, Prof. G. S. Gill)
3 Naval Research Laboratory
    Code 5652
      Dr. J. Caulfield (1)
      Dr. D. Scribner (1)
    Code 6552, Dr. M. Kruer (1)
1 Naval Surface Warfare Center Division, Dahlgren (Code G30-DLB, Brunson)
2 Naval Surface Warfare Center, Dahlgren Division Detachment White Oak, Silver Spring
    Dr. P. Carter (1)
    Dr. R. Cawley (1)
1 Army Missile Command, Redstone Arsenal (AMSMI-RD-GC, Dr. P. Jacobs)
1 Air Force Wright Laboratory, Armament Directorate, Eglin Air Force Base (M. F. Wehling)
1 Defense Advanced Research Projects Agency, Arlington (LTCOL J. Crowley)
2 Defense Technical Technical Information Center, Alexandria
1 Columbia University, Columbia Radiation Laboratory, Department of Electrical
    Engineering, New York, NY (M. C. Teich)
3 Massachussetts Institute of Technology, Lincoln Laboratory, Lexington, MA
    Dr. T. Nguyen (1)
    Prof. A. Willsky (1)
    Dr. G. W. Wornell (1)
1 New York University, Courant Institute of Mathematical Science, New York, NY
    (Prof. S. Mallat)
1 Pennsylvania State University, Applied Research Laboratory, State College, PA
    Dr. J. Hansen)
1 Statistical Sciences, Incorporated, Seattle, WA (Dr. R. D. Martin)
1 University of California, Electrical and Computer Science Department, Santa Barbara, CA
    (Dr. C. Kenney)
1 University of Minnesota, Department of Electrical Engineering, Minneapolis, MN
    (Dr. A. H. Tewfik)